

# **Narrow Band Infrared Filters with Broad Field of View**

Thomas D. Rahmlow, Jr., Jeanne E. Lazo-Wasem, and Edward J. Gratrix  
Rugate Technologies, Inc., 353 Christian Street, Oxford, CT USA 06478-1053

Proc. SPIE 6206, Infrared Technology and Applications XXXII, 62062S (May 18, 2006);  
doi:10.1117/12.683972

Copyright 2019 Society of Photo-Optical Instrumentation Engineers. One print or electronic copy may be made for personal use only. Systematic reproduction and distribution, duplication of any material in this paper for a fee or for commercial purposes, or modification of the content of the paper are prohibited.

# Narrow Band Infrared Filters with Broad Field of View

Thomas D. Rahmlow, Jr., Jeanne E. Lazo-Wasem, and Edward J. Gratrix  
Rugate Technologies, Inc., 353 Christian Street, Oxford, CT USA 06478-1053

## ABSTRACT

Optical interference notch filters shift to shorter wavelengths with increasing angles of incidence. This phenomenon restricts the filter's field of view and limits the practical application of narrow reflection notch filters. The amount of shift is inversely proportional to the effective average index of the composite film. A method of designing narrow notch optical filters with very broad field of view and controllable bandwidth is demonstrated. Because this method produces a filter that is predominantly composed of the high refractive index material, it will shift on angle less than a typical quarter-wave notch filter. Increasing the effective index of the filter also reduces the separation of S and P-polarized light with angle. This paper presents modeled and measured performance for both mid and far-infrared filters developed using this technique. Narrow notch discrete and rugate filter designs are compared.

**Keywords:** interference filter, optical filter, rugate, notch filter, highly asymmetric, thickness modulated

## 1. INTRODUCTION

Optical interference filters are traditionally fabricated by depositing discrete layers of materials of different refractive indices. A simple notch reflector can be fabricated by depositing alternating quarter-wave thick layers of high and low index materials. The bandwidth of the reflection notch is proportional to the index contrast or difference between the high and low indices. In the example of the quarter wave notch filter, the choice of materials determines the bandwidth of the reflection notch. Rugate filters allow for the design of a continuous range of notch bandwidths by controlling the amplitude of the graded index profile. The technique described here uses modulation of the thickness of the discrete layers to achieve the same result. For notch bandwidths of a few percent, the layer thicknesses of one material relative to the other are highly asymmetric and result in an effective refractive index for the full stack that is close to the refractive index of the predominate material. If the high index material is the predominate material, then the shift with angle is reduced to a minimum. The Rugate design will suppress all high order harmonics while the thickness modulated design will exhibit both odd and even harmonics.

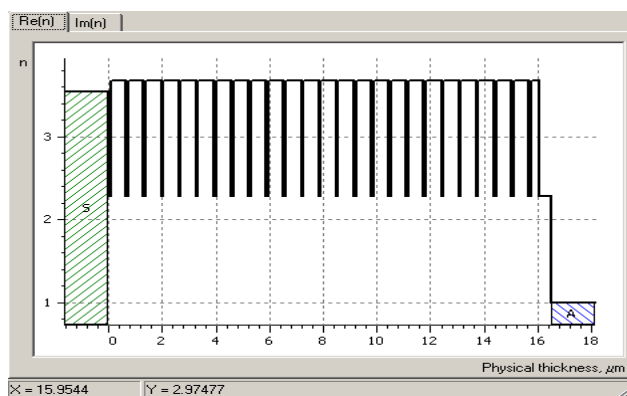


Figure 1: An Asymmetric discrete index profile. In this example, the low index layers are  $1/20^{\text{th}}$  the optical thickness of the high index layers. The OT of the HL group is  $1/2$  the notch center  $\lambda$ . Design materials are Si and ZnS.

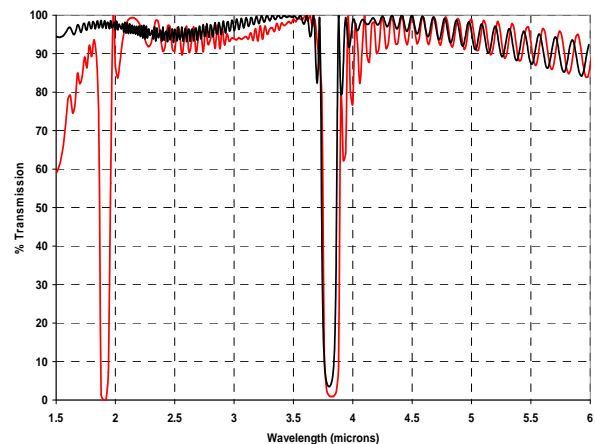


Figure 2: Predicted transmission for an asymmetric notch design and a rugate notch shows the absence of harmonics for the Rugate and the second harmonic for the HAF design. The two filters are designed to similar bandwidths.

Rugate filters are a means of designing narrow reflection notch filters. The index profile is varied as an exponential sine<sup>1</sup>. Controlling the index excursion controls the bandwidth of the reflection notch<sup>2</sup>. The exponential sine wave profile follows the form:

$$n(z)=\exp(1/2[\ln(n_H)+\ln(n_L)]-1/2[\ln(n_H)-\ln(n_L)]\cos(4\pi z/\lambda+\phi)).$$

Where  $n_H$  is the high index,  $n_L$  is the low index,  $\lambda$  is the center wavelength for the reflection notch, and  $z$  is the current optical thickness. The gradient index profile can be fabricated in a number of ways including co-deposition, modulation of film density or control of material stoichiometry<sup>3,4</sup>.

The thickness modulated discrete design described here is a highly asymmetric filter design (HAF). The HAF design uses very thin, low index layers. The spectral position of the reflection band is determined by the optical thickness (OT) of the high-low group. The optical thickness of a group for the HAF design, like that of the quarter wave filter is a half wave of the desired notch location. The optical thickness for the high index layer in the HAF design is nearly half the optical thickness of the desired reflection notch location. The optical thickness of the low index layer is half the optical thickness of the wavelength of the desired notch filter minus the thickness of the high index.

A refractive index profile for an asymmetric notch design is shown in Figure 1. The ratio of the thin layer optical thickness to the thick layer optical thickness is 1/20. Figure 2 illustrates the differences between the predicted transmission spectra between an asymmetric notch filter and a rugate notch filter. Note the absence of the harmonic for the Rugate filter. The discrete filter design is  $(LH)^{24} 0.5L$ .

A thin film's effective index is defined, for s (perpendicular) polarization, as  $n_s = n \cos \alpha$  and, for p (parallel) polarization, as  $n_p = n / \cos \alpha$ <sup>5</sup>. Hence, the film's effective optical thickness decreases with increasing angle. For a notch filter, this implies that the notch will shift to shorter wavelengths with increasing angles of incidence. The amount of shift is inversely proportional to the effective average index of the composite film. Figure 3 shows the notch shift, as a percentage of the notch's center wavelength, as the angle increases, for rugate notch filters of various average indices.

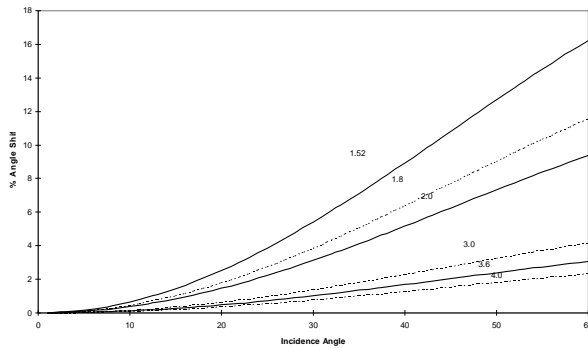


Figure 3: Reflection notches for interference filters shift towards shorter wavelengths as incidence angle is increased from normal to 90. The amount of shift, here a percentage of the notch's center wavelength is a function of average index.

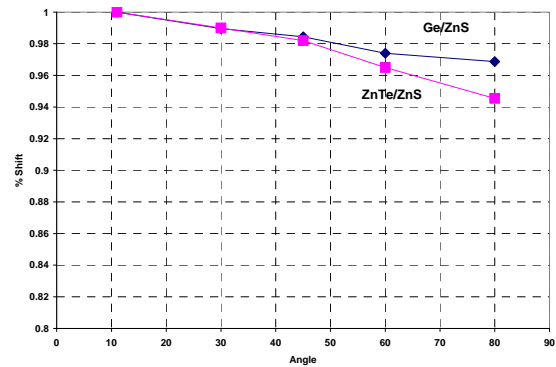


Figure 4: Angle shift, as a percentage of notch location, is shown for two asymmetric notch filters using two different high index materials. Because the low index layers are comparatively thin, the average index of the filter is nearly that of the high index material.

Since the index of the asymmetric filter is dominated by the high index material, the shift on angle is considerably less. Figure 4 shows the relative shift with angle of incidence, for 0.1 ratio HAF designs using different high index materials, Ge and ZnTe. The high refractive index of germanium minimizes the filter's shift with angle. This design shifts less than 4% from normal to 80% AOI. The refractive index of germanium is approximately 4.1 while the index of ZnTe is closer to 3.0.

## 2. DESIGN METHODOLOGY

The highly asymmetric discrete filter design uses very thin, low index layers. The high index layer is nearly  $\frac{1}{2}$  the optical thickness of the desired reflection notch. The basic design formula is that the sum of the low and high index layers equals  $\frac{1}{2}$  the optical thickness of the wavelength of the desired notch filter. This filter design can also be described as a thickness modulated filter design.

### BANDWIDTH

To illustrate, four design examples are considered, this design set varies the thickness of the thin low index layers using thickness ratios of 0.1, 0.05, 0.025 and 0.0125. The model uses Ge as the high and ZnS as the low index material. The number of high/low pairs or groups is increased as the thickness ratio is decreased in order to maintain comparable notch reflection. More groups are required as the thickness ratio is decreased to maintain a desired notch reflection. The four designs are presented in Table 1. Predicted transmission of the design set is presented in Figure 5 through Figure 8. These figures demonstrate that the bandwidth of the notch can be systematically controlled, independent of material selection. Figure 9 shows predicted bandwidth of the narrow reflection notch (FWHM: full width, half maximum). The bandwidth is nearly a linear function of the thickness ratio of the thin layers.

Table 1: Asymmetric Filter Designs

Design ID	Bandwidth	Layers	Thickness	Design
A	7.8% (0.10)	62	15.3/58	(0.1L1.9H) <sup>30</sup> 0.75L 0.75A
B	4.1% (0.05)	92	22.1/87	(0.05L1.95H) <sup>45</sup> 0.75L 0.75A
C	2.1% (0.025)	182	42.9/172	(0.025L1.975H) <sup>90</sup> 0.75L 0.75A
D	1.2% (0.0125)	362	84.6/343	(0.0125L1.9875H) <sup>180</sup> 0.75L 0.75A

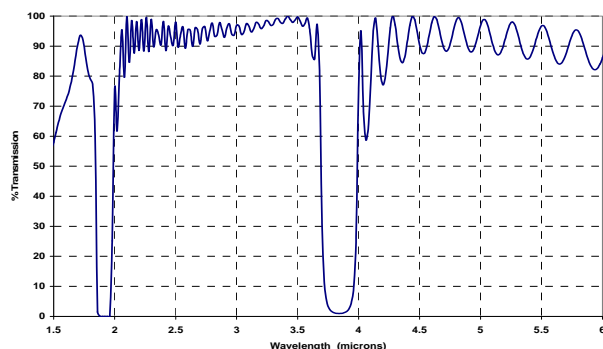


Figure 5: Design A (0.1L1.9H)<sup>30</sup> 0.75L 0.75A

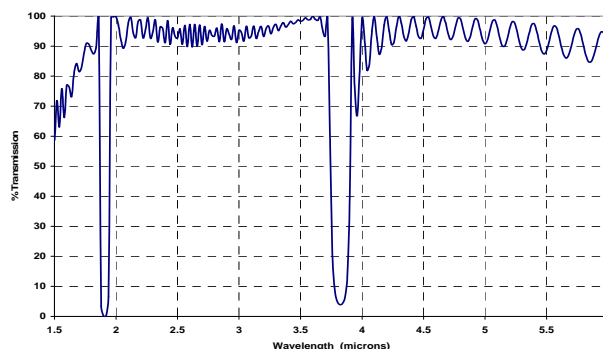


Figure 6: Design B (0.05L1.95H)<sup>45</sup> 0.75L 0.75A

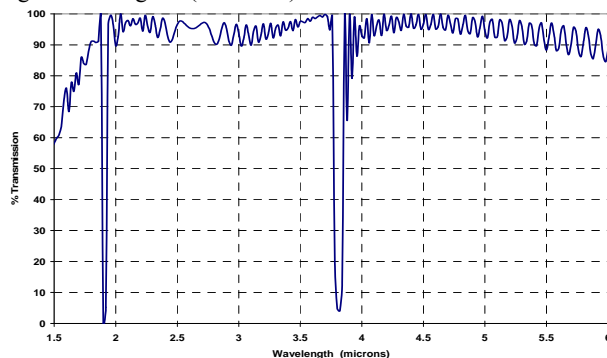


Figure 7: Design C (0.025L1.975H)<sup>90</sup> 0.75L 0.75A

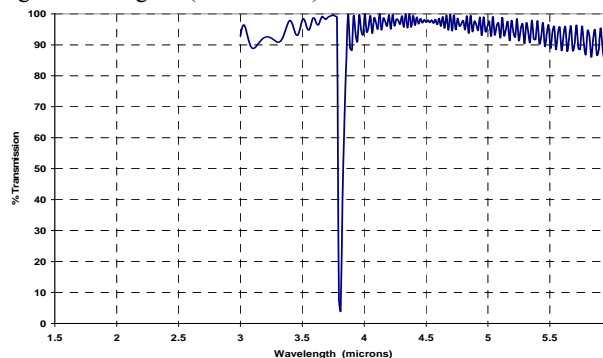


Figure 8: Design D (0.0125L1.9875H)<sup>180</sup> 0.75L 0.75A

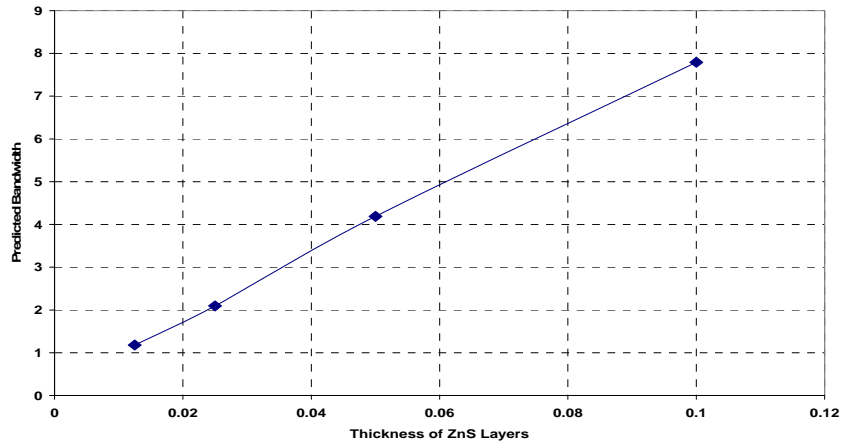


Figure 9: The notch bandwidth of the asymmetric design varies smoothly with the optical thickness of the thin low index layers. The focus of this paper is narrow notch filter design. In fact, the bandwidth varies smoothly (though not linearly) from the quarter wave thickness to these highly asymmetric thin layers<sup>6</sup>.

### FIELD OF VIEW

Predicted performance of the same designs in Table 1 was calculated at various angles of incidence, from normal to 80°. Figures 10 through 13 present predicted performance for the filter set at normal and at the angle of maximum coverage.

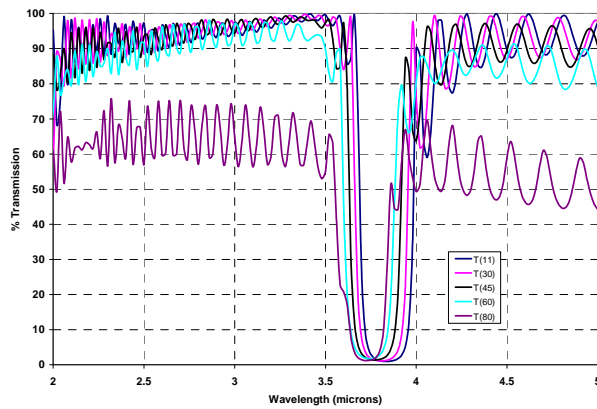


Figure 10: 8% bandwidth notch provides angle coverage from normal to 80° AOI.

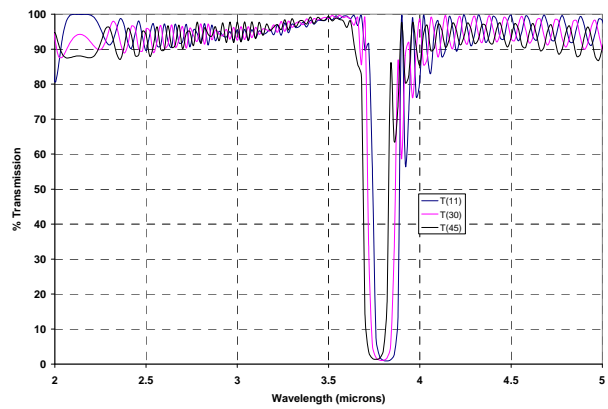


Figure 11: 4% bandwidth notch provides angle coverage from normal to 45° AOI

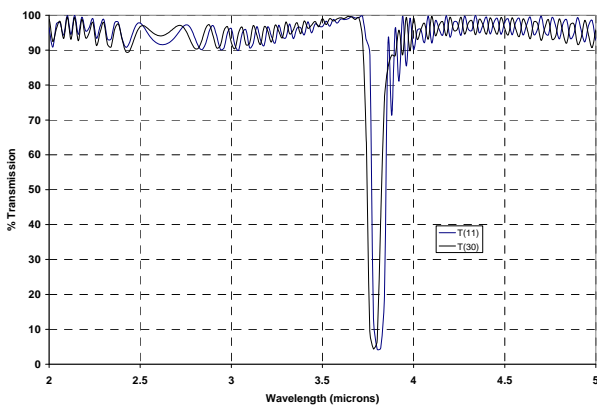


Figure 12: 2% bandwidth notch provides angle coverage from normal to 30° AOI.

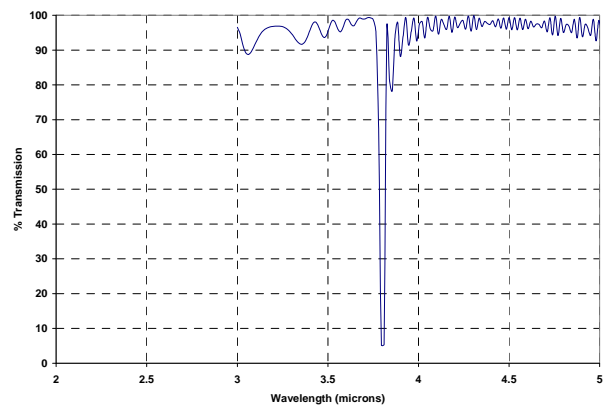


Figure 13: 1.2% bandwidth notch provides angle coverage from normal to 12° AOI.

## POLARIZATION

Polarization issues are a concern when considering the performance of a notch filter at angle. At normal incidence, the filter reflects S and P polarized light equally. S and P polarization performance separate as the angle of incidence (AOI) is increased away from normal. The average performance is the average of S and P performance. Increasing the effective index of the filter reduces the separation of S and P with angle. Figure 14 through 18 present predicted notch performance from 0 to 80° AOI. The greatest separation of S and P transmission at high AOI occurs in the passband rather than the reflection notch. This is due to the use of low index material in the final filter-to-air matching layers.

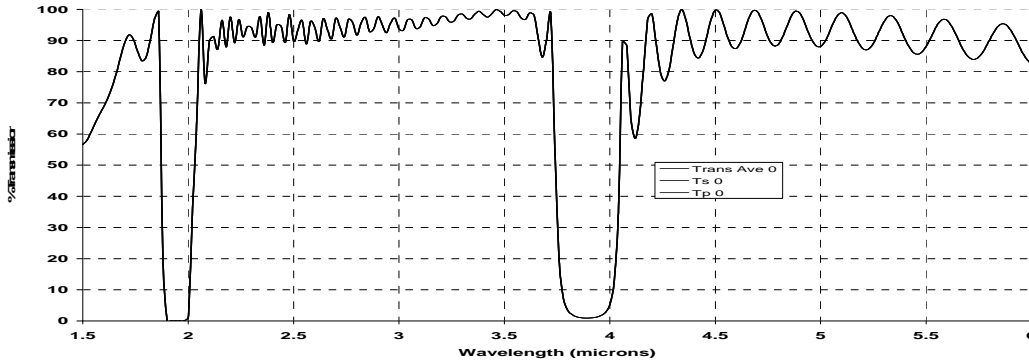


Figure 14: Normal AOI S, P and average transmission for a 0.1 (A) thickness modulated, Ge/ZnS notch filter .

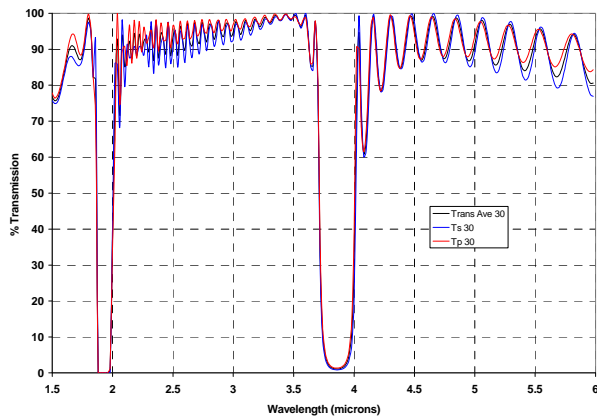


Figure 15: 30° AOI S, P and average transmission for a 0.1 (A) thickness modulated, Ge/ZnS asymmetric notch filter

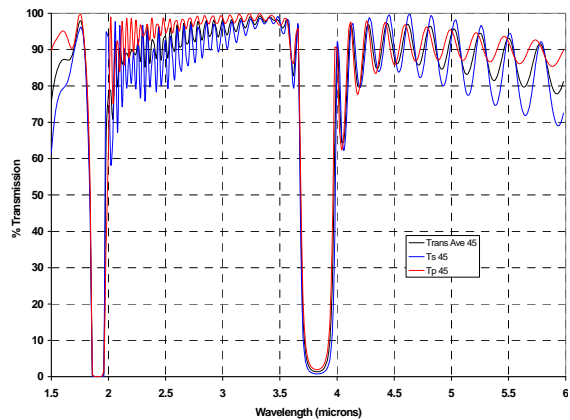


Figure 16: 45° AOI S, P and average transmission for a 0.1 (A) thickness modulated, Ge/ZnS asymmetric notch filter

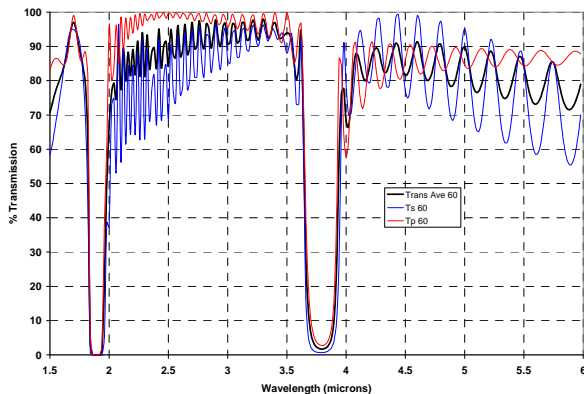


Figure 17: 60° AOI S, P and average transmission for a 0.1 (A) thickness modulated, Ge/ZnS asymmetric notch filter

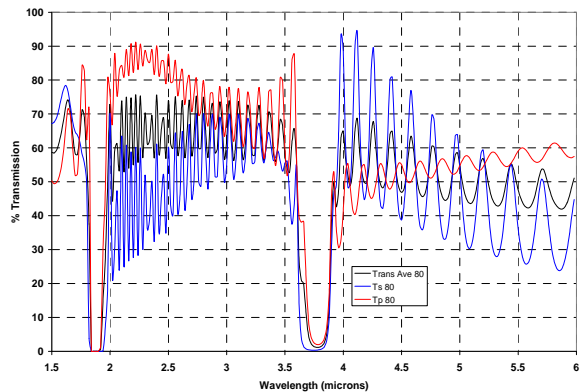


Figure 18: 80° AOI S, P and average transmission for a 0.1 (A) thickness modulated, Ge/ZnS asymmetric notch filter

### 3. FILTER FABRICATION

Discrete filter fabrication consists of depositing independent layers of high and low index materials (Figure 19). Fabrication of high optical density notch filters in the infrared is a lengthy process requiring large source material capacity, sophisticated monitoring and control techniques, and well understood material properties. Uniformity control techniques must be in place in order to fabricate large filters or larger quantities of filters. The resulting thick films must be free of defects and residual stress. Far infrared filters can require deposition times exceeding 16 hours.

The filters reported on here were deposited using standard physical vapor deposition techniques (PVD), either electron-beam, resistive (thermal), or a combination of both. Multiple quartz crystal monitors are used to determine the thickness of each layer. Computer software automatically controls the entire filter deposition. It ramps and soaks the source material, opens shutters and deposits the layer, analyzes crystal thickness data, and terminates each layer. Audio feedback alerts nearby operators if manual assistance is required.

The highly asymmetric design can be deposited as independent layers of high and low index materials or the low index layers can be rapidly blended in. The advantage of rapidly blending in the low index materials is that the process can continue without interruption. The blending of the low index layers can shorten the total deposition time (Figure 20).

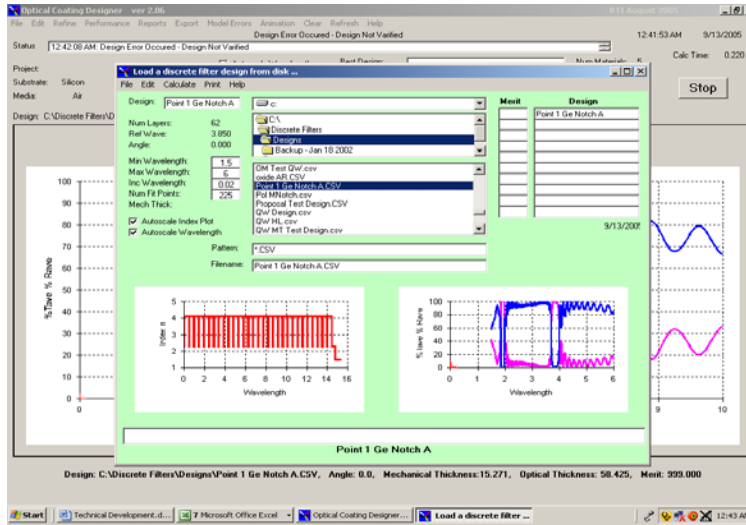


Figure 19: As a discrete filter, the layers can be deposited as individual layers. Deposition time is approximately 30 minutes per group for a 3.8 μm notch.

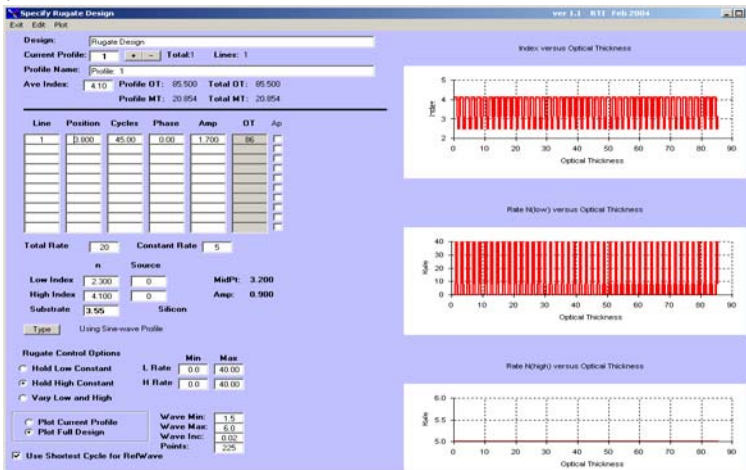


Figure 20: The high index material can be deposited at a constant uninterrupted rate and the low index can be turned on and off. Deposition time can be cut to 15 minutes per group.

## 4. RESULTS

Mid and far infrared notch filters have been designed and fabricated using the highly asymmetric techniques described here. Predicted and measured transmission for a MIR notch filter at  $4.2\mu\text{m}$  is shown in Figure 21. Its measured optical density, at angles of incidence from normal to  $60^\circ$ , is shown in Figure 22. This filter is a 1/10 ratio design using ZnS and Ge.

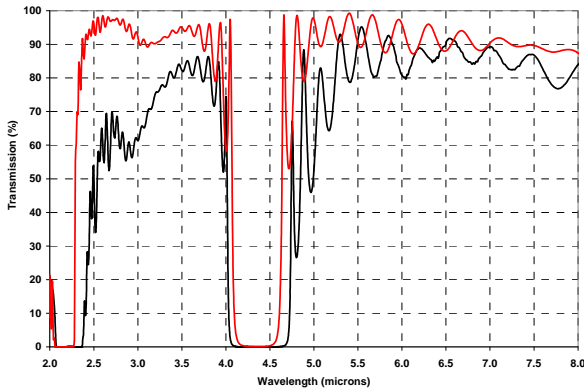


Figure 21: Overlay of predicted and measured transmission for a  $4.2\mu\text{m}$  asymmetric notch Ge/ZnS notch filter at normal AOI.

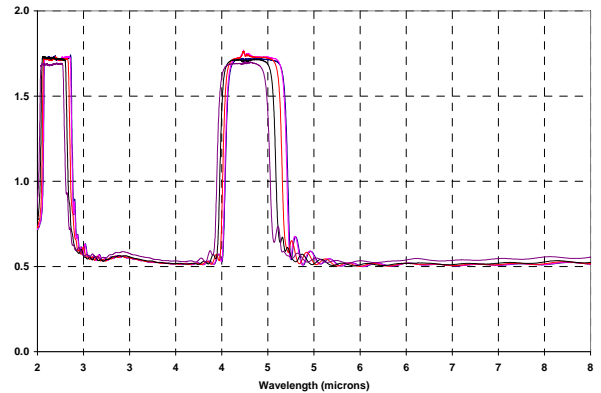


Figure 22: Overlay of measured optical density for the  $4.2\mu\text{m}$  notch filter at 0, 11, 30, 45 and 60 AOI. (S2 is not AR coated).

Measured transmission for three mid-IR notch filters is presented in Figure 23. The ratio of optical thickness for these filter is 1/10, 1/20 and 1/40. Measured transmission for two far-IR notch filters are presented in figure 24. The optical thickness ratio for these filters is 1/10 and 1/20. These plots demonstrate control of bandwidth using the HAF design method.

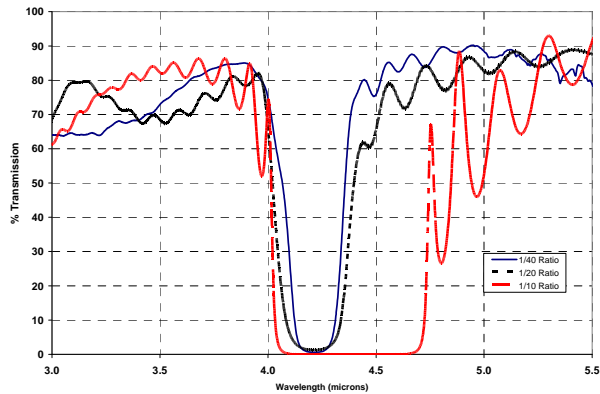


Figure 23: Overlay of measured transmission for 1/10 (dash dot), 1/20 (dashed) and 1/40 index ratio ZnS/Ge discrete notch filters.

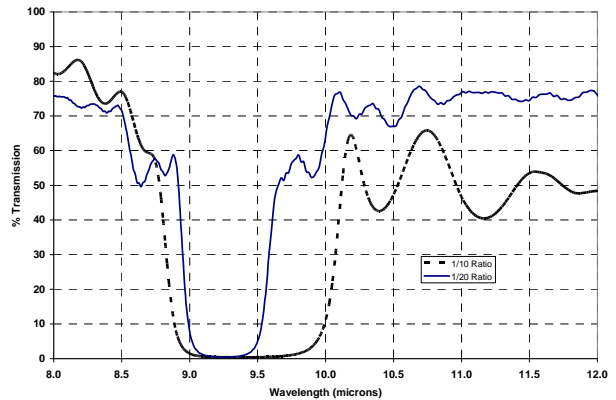


Figure 24: Overlay of measured transmission for 1/10 (dashed) and 1/20 index ratio ZnS/Ge discrete notch filters.



## 5. CONCLUSIONS

Angle shift to shorter wavelengths has generally limited the use of narrow notch filters to systems that offer limited field of view or high numerical aperture. This design approach maximizes the effective index of the discrete film stack and thus minimizes the impact of angle shift. An 8% bandwidth Ge/ZnS filter can effectively block a fixed laser wavelength from normal to better than 80° angle of incidence. A 4% bandwidth filter can cover normal to 45° angle of incidence. The narrow filter design maximizes spectral throughput while providing high optical density in the rejection band.

Narrow notch reflection filters are appropriate for a range of applications including sensor laser protection, suppression of background light between adjacent missile warning bands or selective reflection of specific wavelengths to improve a retro-reflected signal to ambient light levels. Designing filter bandwidths to meet system specific requirements of field of view while maintaining high transmission in the passband regions is a challenge. This design technique allows for bandwidth control and high angle stability. The discrete HAF filter is approximately 30% thinner in physical thickness than a rugate notch designed to the same bandwidth and notch optical density. While the HAF designs exhibit high order harmonics, they perform well for single spectral band use (3 -5 or 7 to 14 microns).

We have fabricated several example filters and their measured performance compares well with modeled performance. The filters are relatively thick, consisting of 80 layers or more to achieve high optical densities, but standard discrete deposition techniques can be used.

## REFERENCES

1. P. Baumeister, *Optical Coating Technology*, SPIE Press, pp. 5-27, 2004.
2. W. Southwell, "Spectral response calculations of rugate filters using coupled wave theory", *JOSA*, Vol. 5, No. 9, pp. 1558-1564, 1988.
3. Rahmlow, T.D., and Lazo-Wasem, J.E., "Process design issues for rugate coating fabrication", SVC annual meeting, SVC, O-20 (1998).
4. Rahmlow, T.D. and Lazo-Wasem, J.E., "Rugate and discrete hybrid filter designs", SPIE Annual Conference, SPIE, 33104, (1997).
5. Macleod, H., *Thin-Film Optical Filters*, 3<sup>rd</sup> edition, IoP Press, 2001
6. P. Baumeister, *Optical Coating Technology*, SPIE Press, pp. 5-13, 2004.